Est. 1984

ORIENTAL JOURNAL OF CHEMISTRY
An International Open Free Access, Peer Reviewed Research Journal

www.orientjchem.org

ISSN: 0970-020 X
CODEN: OJCHEG
2016, Vol. 32, No. (1):
Pg. 637-649

Structure and Nonlinear Optical Properties Study of 2-Amino-5-Chlorobenzophenone: (A Spectroscopic Approach)

C. JESINTHA JOHN[1,2], D. MANIMARAN[1], I. HUBERT JOE[1]*, GEORGE LUKOSE[3] and SHERIFA RAHIM[4]

[1]Department of Physics, Mar Ivanios College, Thiruvananthapuram-695015, Kerala, India.
[2]Department of Physics, St. Joseph's College for Women, Alappuzha-688001, Kerala, India.
[3]Department of Chemistry, Mar Ivanios College,Thiruvananthapuram-695015, Kerala, India.
[4]Department of Chemistry, St. John's College, Anchal, Kollam-691306, Kerala, India.
*Corresponding author E-mail: hubertjoe@gmail.com

http://dx.doi.org/10.13005/ojc/320172

Received: January 13, 2016; Accepted: February 18, 2016

ABSTRACT

The FT-IR and FT-Raman spectra of 2-amino-5-chlorobenzophenone have been recorded and analyzed. Structural geometry, vibrational wavenumbers and first-order hyperpolarizability were computed using density functional theory method. N-H···O distance shows the possibility of intramolecular hydrogen bonding. Natural bond orbital analysis confirms the presence of the N-H···O hydrogen bonding. The computed first-order hyperpolarizability value suggests that 2-amino-5-chlorobenzophenone has a potential for producing the second harmonic generation.

Key words: Vibrational spectra, Density functional theory, Natural bond orbital, Hydrogen bonding, Hyperpolarizability.

INTRODUCTION

Benzophenone, an aromatic ketone (diphenylketone), is an important compound in organic photochemistry which is used as a constituent of synthetic perfumes and as a starting material for the manufacture of dyes, pesticides and drugs and also used as a photo initiator of UV-curing applications in inks, adhesive and coatings, optical fiber as well as in printed circuit boards. It has been the object of many spectral, structural and theoretical investigations because of its interesting chemical and physical properties. Further, the crystals of benzophenones are found to be useful materials for the fabrication of nonlinear optical devices [1,2]. A number of benzophenone derivatives show significantly high second harmonic generation conversion efficiency [3-5].

The present study deals with the vibrational analysis of 2-amino-5-chlorobenzophenone (2A-5CB) using density functional theory (DFT)

calculations [6] to elucidate the correlation between the molecular structure, nonlinear optical (NLO) property, charge transfer interactions, and first-order hyperpolarizability.

MATERIALS AND METHODS

The commercially available 2A-5CB ($C_{13}H_{10}ClNO$) was purified by repeated recrystallization process using ethanol. Since the solubility of 2A-5CB is high (10.65 gm/100 ml of ethanol at 35°C) in ethanol, it is easy to grow good quality single crystal. The seed crystals were obtained after three days, among them the defect free and perfectly shaped ones with high transparency were used as the seed crystals for further growth experiment. The seed crystals were first seasoned in the mother solution taken in the Mason jar crystallizer using nylon thread and then allowed to grow into bigger size. The jar was covered with perforated lid to facilitate the slow evaporation of the solvent at a constant temperature of 305K. Single crystals of size 14 x 6 x 5 mm^3 are grown in a period of 50-60 days. The crystals tend to grow as needles and appear dark gold in color with good transparency.

$$I_i = \frac{f(\nu_o - \nu_i)^4 S_i}{\nu_i \left[1 - \exp\left(\frac{-hc\,\nu_i}{kT}\right)\right]} \quad ...(1)$$

The room temperature FTIR spectra of the title compound was recorded in the region 4000-400 cm^{-1} at a resolution of ±1 cm^{-1}, using Bruker IFS 66V vacuum Fourier transform spectrometer, a KBr beam splitter and globar source. The FT-Raman spectra were recorded on the same instrument with FRA 106 Raman accessories in the region 3500-50 cm^{-1}. Nd:YAG laser operating at 200 mW power with 1064 nm excitation source.

DFT performed using Gaussian'09 program [7] at the B3LYP level [8,9], with 6-31G(d) basis set has been used to compute molecular structure and vibrational wavenumbers. For the plots of simulated IR and Raman spectra, pure Lorentzian band shapes were used with full width at half maximum band width of 10 cm^{-1}. The calculated Raman activities were converted to relative Raman intensities using the following relationship derived from the basic theory of Raman scattering [10,11].

where, μ_o is the exciting frequency (in cm^{-1}), μ_i the vibrational wavenumber of the i^{th} normal mode, h, c and k, the universal constants and f is the suitably chosen common scaling factor for all the peak intensities.

RESULTS AND DISCUSSION

Molecular geometry study

The optimized molecular structure of 2A-5CB was calculated at B3LYP/6-31G(d) level of theory. The optimized molecule structure is shown in Fig. 1. The geometrical parameters are tabulated in Table 1.

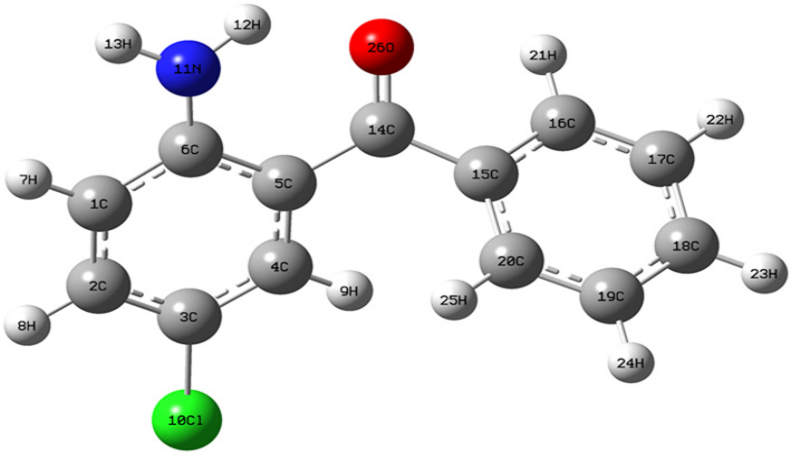

Fig. 1: Optimized structure of 2A-5CB

The dihedral angle C_5-C_6-N_{11}-H_{12} of the amino group with the phenyl ring 1 shows a deviation of 18.51° from the plane of the ring. The internal bond angle at the carbon atom to which amino group attached (C_1-C_6-C_5=118.286 Å) is consistently smaller than the normally adopted internal bond angle of the phenyl ring. The tri-substituted benzene ring appears a little distorted with C_5-C_6 and C_1-C_6 bond lengths 1.43118 and 1.41395 Å, respectively exactly at the amino group substitution which are longer than C_3-C_4, C_2-C_3 and C_1-C_2 bond lengths 1.3831, 1.40 and 1.3853 Å, respectively. These indicate the resonance effect between the amino group and the phenyl ring1. The bond angle of carbon atom attached to the chlorine atom (C_2-C_3-C_4=120.24 Å) exceeds the normal value 120°. This is due to the electron donating nature of the chlorine atom.

Table 1: The optimized geometrical parameters of 2A-5CB at DFT level of theory

Bond length (Å)		Bond angles (º)		Dihedral angles (º)	
Parameters	**value**	**Parameters**	**value**	**Parameters**	**value**
C1-C2	1.383	C1-C2-C3	119.6	C1-C2-C3-C4	1.2
C2-C3	1.400	C2-C3-C4	120.2	C2-C3-C4-C5	-0.25
C3-C4	1.383	C3-C4-C5	121.3	C3-C4-C5-C6	-1.87
C4-C5	1.459	C4-C5-C6	118.8	C3-C2-C1-H7	179.16
C5-C6	1.410	C2-C1-H7	119.6	C4-C3-C2-H8	-179.61
C1-H7	1.087	C3-C2-H8	120.0	C2-C3-C4-H9	-178.69
C2-H8	1.085	C3-C4-H9	119.3	C1-C2-C3-Cl10	-178.55
C4-H9	1.082	C2-C3-Cl10	119.7	C4-C5-C6-N11	-179.26
C3-Cl10	1.762	C5-C6-N11	121.9	C5-C6-N11-H12	18.51
C6-N11	1.365	C6-N11-H12	116.3	C5-C6-N11-H13	168.67
N11-H12	1.013	C6-N11-H13	118.2	C3-C4-C5-C14	-178.62
N11-H13	1.009	C4-C5-C14	120.6	C4-C5-C14-C15	-20.89
C5-C14	1.483	C5-C14-C15	120.9	C5-C14-C15-C16	145.84
C14-C15	1.502	C14-C15-C16	117.8	C14-C15-C16-C17	176.83
C15-C16	1.403	C15-C16-C17	120.5	C15-C16-C17-C18	-1.55
C16-C17	1.391	C16-C17-C18	120.1	C16-C17-C18-C19	0.05
C17-C18	1.398	C17-C18-C19	119.9	C17-C18-C19-C20	1.05
C18-C19	1.395	C18-C19-C20	120.1	C18-C17-C16-H21	178.33
C19-C20	1.395	C17-C16-H21	120.8	C19-C18-C17-H22	179.55
C16-H21	1.085	C18-C17-H22	120.1	C16-C17-C18-H23	-179.51
C17-H22	1.086	C17-C18-H23	120.1	C17-C18-C19-H24	-178.79
C18-H23	1.086	C18-C19-H24	120.2	C18-C19-C20-H25	-178.94
C19-H24	1.086	C19-C20-H25	119.7	C16-C15-C14-O26	-34.25
C20-H25	1.085	C15-C14-O26	117.7		
C14-O26	1.237				

Conjugation of carbonyl group with the phenyl rings would favour a planar conformation, but the steric repulsion between the two *ortho* hydrogen atoms H_9 and H_{25} prevents the attainment of co-planarity [12]. The two phenyl rings of 2A-5CB are non-planar with C_6-C_5-C_{14}-C_{15} (162.42 Å) and C_5-C_{14}-C_{15}-C_{16} (145.84 Å) dihedral angles. This behaviour has been observed in many structural and spectroscopic studies of diphenyl compounds [13]. The C_5-C_{14} (1.483) and C_{14}-C_{15} (1.5027 Å) are slightly larger than other C-C bonds, indicating negligible conjugation interaction between the two phenyl ring

systems. The short inter-atomic distance N_{11}-H_{12}···O_{26} reveals the possibility of intramolecular hydrogen bonding.

Potential energy surface scan study

In order to reveal the minimum energy conformation of the compound, the detailed potential energy surface scan of the dihedral angle C_5-C_{14}-C_{15}-C_{16} is performed. The scan has been carried out by minimizing the potential energy in all geometrical parameters by changing the torsion angle for every 10° for a 360° rotation. The shape of the potential energy as a function of the dihedral angle is illustrated in Fig. 2.

The structural studies of tri-substituted benzophenone show approximately equal twist angles of each ring in the range of 20-35°. Hence, a subsequent geometry optimization calculation was carried out by allowing the rotation around the two phenyl rings. From the Fig. 2, it can be shown that the global minimum is observed at 30°. The global minimum energy obtained to be -1091.61 kJ mol^{-1}.

Natural bond orbital analysis

The natural bond orbital (NBO) analysis provides a description of the structure of a conformer by a set of localized bond, antibonds and Rydberg extra valence orbitals. Stabilizing interactions between filled and unoccupied orbitals and destabilizing interactions between filled orbitals can also be obtained from this analysis [14-16]. Therefore, NBO theory is a valuable complement to the energetic and structural data. DFT level computation is used to investigate the various second order interactions between the filled orbitals of one subsystem and the vacant orbitals of another subsystem, which is a measure of delocalization or hyperconjugation[17]. The main natural orbital interactions were analyzed with the NBO 3.1 program [18]. The hyperconjugative interaction energy was deduced from the second-order perturbation approach.

$$E(2) = -n_\sigma \frac{\langle \sigma | F | \sigma \rangle^2}{\varepsilon_{\sigma^*} - \varepsilon_\sigma} = -n_\sigma \frac{F_{ij}^2}{\Delta E} \quad ...(2)$$

where, <σ|F|σ< is the Fock matrix element between i and *j* NBO orbitals, σ_s and n_{σ^*} are the energies of s and σ* NBO's, and n_s is the population of the donor s orbital. NBO theory can also be used to identify the hydrogen bonding.

The lowering of orbital energy due to the interaction between doubly occupied orbitals and unoccupied ones is a convenient guide to interpret the molecular structure in the electronic point of view. In energetic terms, hyperconjugation is an important effect in which an occupied Lewis-type natural bond orbital is stabilized by overlapping with a non Lewis-type orbital (either one-center Rydberg or two-center antibonding NBO). This electron delocalization can be described as a charge transfer from a Lewis valence orbital (donor), with a decreasing of its occupancy, to a non-Lewis orbital (acceptor). NBO analysis of 2A-5CB has been performed in order to elucidate the bond effect, intramolecular N-H···O hydrogen bonding and hyperconjugative interaction and the results are shown in the Tables 2 and 3.

The N-H···O hydrogen bonding, in NBO terms, corresponds to the oxygen lone pair and the electron transfer from LP oxygen to the antibonding (N-H) orbital. The energy lowering corresponding to the interaction between a filled orbital (i) and an antibonding orbital (j*), is deduced from the second-order perturbation of the filled orbital. Among the most energetic donor–acceptor NBO interactions are those involving the p-type lone pair of the oxygen atom, LP_2O_{26} with vicinal $\pi^*(N_{11}$-$H_{12})$ antibonds having energy contribution 32.3 kJ mol^{-1} of hyperconjugative interaction is weak, these E(2) values and the low value electron density (0.5181e) are chemically significant and can be used as a measure of the intramolecular delocalization. The energy values

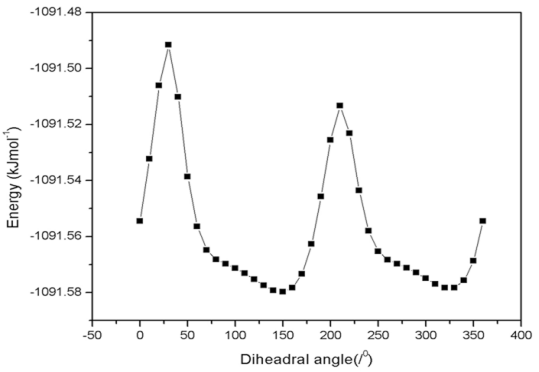

Fig. 2: Potential energy surface scan curve for the dihedral angle C5-C14-C15-C16

corresponding to the charge transfer in the molecules are formed by hydrogen bonding.

The intramolecular hyperconjugative interactions are formed by the orbital overlap between π(C-C) and π*(C-C) bond orbitals, which results in intramolecular charge transfer (ICT) causing stabilization of the system. These interactions are observed as an increase in ED in C-C anti-bonding orbital that weakens their respective bonds. The ED at the six conjugated π(C-C) bonds (1.6-1.7e) and π* bonds (0.213-0.464e) of the phenyl rings clearly demonstrate strong delocalization of electrons leading to a stabilization of energy (80-90 kJ mol^{-1}). This is due to intramolecular charge transfer interaction inside the ring. Among the most energetic donor-acceptor NBO interactions are those involving the *p*-type lone pair of the oxygen atom, LP_1N_{11} with $\pi^*(C_5\text{-}C_6)$ antibonds and, LP_3Cl_{10} with $\pi^*(C_3\text{-}C_4)$ having energy contributions 180.71 and 46.52 kJ mol^{-1}, respectively of hyperconjugative interaction are chemically significant and can be used as a measure of the intramolecular delocalization. A strong interaction has also been observed between the *p* type orbital containing the lone electron pair of O_{26} and the neighbourhood anti-bonding orbitals $\sigma^*(C_5\text{-}C_{14})$ and $\sigma^*(C_{14}\text{-}C_{15})$, respectively. This interaction is responsible for hyperconjugation

Table 2: NBO result showing the formation of Lewis and non-Lewis orbitals by the valance hybrids corresponding to the intramolecular N-H...O

Bond(A-B)	ED (a.u)	EDA%	EDB %	NBO	S%	P%
π C18-C19	1.6527	49.18	50.82	$0.7013(sp1.00)_C$	0.00	99.96
	-0.2495	-	-	$0.7129(sp1.00)_C$	0.00	99.96
π C16-C17	1.6559	48.56	51.44	$0.7081(sp1.81)_C$	35.58	64.38
	-0.2481	-	-	$0.7061(sp1.83)_C$	35.26	64.7
π C15-C20	1.645	51.86	48.14	$0.7202(sp99.99)_C$	0.01	99.96
	-0.2499	-	-	$0.6938(sp99.99)_C$	0.03	99.93
π C14-O26	1.9691	31.44	68.56	$0.5607(sp99.99)_C$	0.03	99.8
	-0.3686	-	-	$0.8280(sp99.99)_O$	0,04	99.68
π C5-C6	1.5731	58.78	41.22	$0.7667(sp99.99)_C$	0.01	99.98
	-0.2473	-	-	$0.6420(sp1.00)_C$	0.00	99.96
π C1-C2	1.7277	53.9	46.1	$0.7342\ (sp1.00)_C$	0.00	99.96
	-0.2608	-	-	$0.6790(sp1.00)_C$	0.00	99.94
π C3-C4	1.7225	56.06	43.94	$0.7488(sp1.00)_C$	0.00	99.98
	-0.2702	-	-	$0.6628(sp1.00)_C$	0.00	99.95
π*C3-C4	0.3687	43.94	56.06	$0.6628(sp1.00)_C$	0.00	99.98
	0.0194	-	-	$-0.7488(sp1.00)_C$	0.00	99.95
π*C1-C2	0.3039	46.1	53.9	$0.6790\ (sp1.00)_C$	0.00	99.96
	0.0282	-	-	$-0.7342\ (sp1.00)_C$	0.00	99.94
π*C5-C6	0.4642	41.22	58.78	$0.6420(sp99.99)_C$	0.01	99.98
	0.0191	-	-	$-0.7667(sp1.00)_C$	0.00	99.96
π*C16-C17	0.297	51.44	48.56	$0.7172\ (sp1.00)_C$	0.00	99.95
	-0.0363			$-0.6969\ (sp1.00)_C$	0.00	99.96
π*C15-C20	0.3658	48.14	51.86	$0.6938(sp99.99)_C$	0.01	99.96
	0.0313	-	-	$-0.7202(sp99.99)_C$	0.03	99.93
π*C14-O26	0.2133	68.56	31.44	$0.8280\ (sp99.99)_C$	0.03	99.8
	0.0092	-	-	$-0.5607(sp99.99)_O$	0.04	99.68
π*C18-C19	0.3213	50.82	49.18	$0.7129\ (sp1.00)_C$	0.00	99.96
	0.0319	-	-	$-0.7013\ (sp1.00)_C$	0.00	99.96
π*N11-H12	0.03183	26.84	73.16	$0.5181\ (sp2.3)_N$	30.3	69.64

between O_{26} and the ring. These ICT results support the nonlinear optical activity of the molecule.

Vibration spectral analysis

The observed and calculated wavenumbers together with the calculated IR and Raman intensities are assigned based on potential energy distributions (PED) using VEDA4 program [19], which are given in table 4. The observed and simulated vibrational spectra are presented in Figs. 3 and 4. The spectra consists of vibrational patterns originating from the mono and tri-substituted benzene rings and also the

Table 3: Second order perturbation theory analysis of Fock matrix in NBO basis

Donor NBO (i)	ED (i) e	Acceptor NBO (j)	ED (j) e	E(2) kJ/ mola	E(j)-E(i) kJ/ mola	F (i,j) kJ/ mola
π(C1-C2)	1.7277	π* (C3-C4)	0.36870	62.5	735.1	154.9
		π*(C5-C6)	0.46418	90.9	735.1	191.7
π(C3-C4)	1.7225	π*(C1-C2)	0.30394	92	787.7	191.7
		π*(C5-C6)	0.46418	52.1	761.4	147
π(C5-C6)	1.5731	π*(C1-C2)	0.30394	58.7	735.1	149.7
		π*(C3-C4)	0.36870	113.2	708.9	202.2
π(C15-C20)	1.6450	π*(C14-C26)	0.21333	59.5	682.6	147
		π*(C16-C17)	0.29702	82.2	761.4	178.5
		π*(C18-C19)	0.32134	79.9	735.1	173.3
π(C16-C17)	1.6559	π*(C15-C20)	0.36582	81.3	735.1	173.3
		π*(C18-C19)	0.32134	88.6	735.1	181.2
π(C18-C19)	1.6527	π*(C15-C20)	0.36582	89.8	735.1	183.8
		π*(C16-C17)	0.29702	77.2	761.4	173.3
LP1 N11	1.7538	π*(C5-C6)	0.46418	180.7	761.4	275.7
LP2 O26	1.8851	σ*(C5-C14)	0.05521	62.8	1916.6	249.4
		σ*(C14-C15)	0.05987	77.9	1837.9	273.1
		σ*(N11-H12)	0.03183	32.3	1995.4	183.8
LP3 Cl10	1.9427	π*(C3-C4)	0.36870	46.52	866.6	154.9

[a]E(2) means energy of hyperconjugative interactions (stabilization energy)
[b]Energy difference between donor and acceptor i and j NBO orbitals
[c]F(i, j) is the Fock matrix element between i and j NBO orbitals

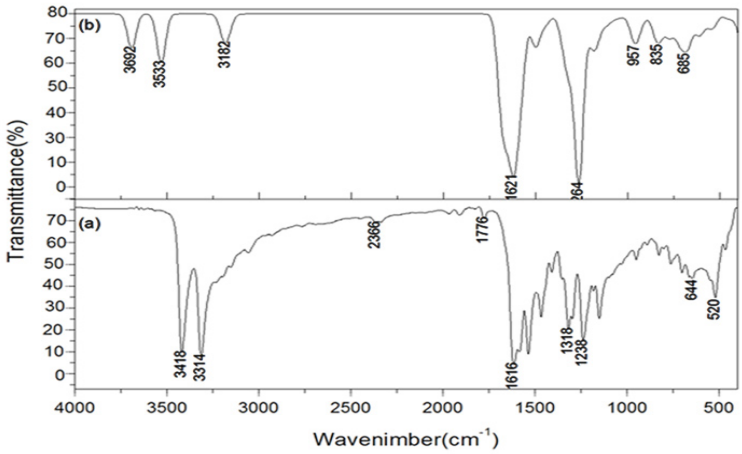

Fig. 3: (a) Experimental (b) simulated infrared spectra of 2A-5CB

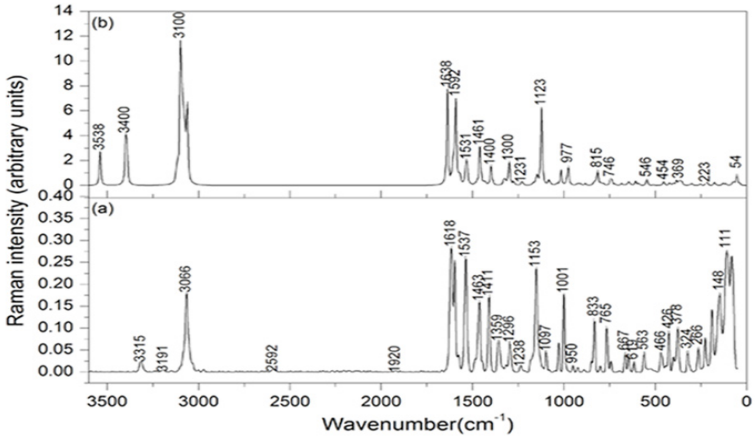

Fig. 4: (a) FT-Raman (b) simulated Raman spectra of 2A-5CB

spectral lines corresponding to CO, NH_2 and CCl group vibrations that are discussed.

Phenyl ring vibrations

2A-5CB consists of an asymmetrically tri-substituted (Ph_1) and a mono-substituted benzene ring (Ph_2). The various normal modes of vibrations of these rings are assigned according to Wilson's numbering convention [20,21] which are well shown in the calculated DFT level.

An asymmetric tri-substituted aromatic system (Ph_1) has two adjacent and one isolated C-H moieties. The hetero aromatic structure shows the presence of C-H stretching vibrations in the region 3100-3000 cm^{-1}, which is the characteristic region for the ready identification of C-H stretching vibration which are 2, 20a and 20b modes. Only ring mode 2 is observed in Raman as a weak band at 3191 cm^{-1} (PED 99%). The bands 20a and 20b are absent or mixed with other bands and cannot be distinctly observed. These wavenumbers do not correlate with the experimental band position and can be substituted to the intermolecular non bonded interactions. Also ring modes are found to be sensitive to other interactions and the shifting of band position of these modes can be observed. In the case of mono-substituted phenyl ring (Ph_2), there are five C-H stretching vibrations active. They are 2,7a,7b,20a and 20b, which fall in the region 3120-3010 cm^{-1} [22]. The weak shoulder band in IR at 3063 cm^{-1} and the strong band at 3066 cm^{-1} in Raman are assigned to the 20a mode, the PED being 87%. Several C-H stretching modes are found to be weak, which are due to the charge transfer between the hydrogen atoms and the carbon atoms [23].

Normal vibrations 8a, 8b, 19a, 19b and 14 are categorized as C-C stretching vibrations in phenyl ring [24]. The mode 8a of the mono-substituted ring vibrations usually appears in the region 1614-1575 cm^{-1} and 8b mode extends around 1597-1562 cm^{-1}. The normal mode 8a is found at higher wavenumber than 8b and appears as a strong band in Raman at 1596 cm^{-1} (PED 61%). The mode 8b of the mono-substituted ring Ph_2 is also observed in Raman as a weak shoulder band at 1575 cm^{-1}. The vibrational modes 19b, 19a and 14 of ring1 are computed at 1534, 1459 and 1398 cm^{-1}, respectively and the band at 1326 cm^{-1} also has contribution from mode 14. The mode 19b is found to be a strong band at 1536 in IR and at 1537 cm^{-1} in Raman while for 19a, a weak band at 1466 cm^{-1} in IR and a strong band at 1464 cm^{-1} are observed. Vibration 14 can be observed as a medium band in IR at 1405 cm^{-1} and as a strong band in Raman at 1410 and a medium band at 1359 cm^{-1}. The simultaneous appearance of the ring C-C stretching bands in both IR and Raman modes of 19a, 19b and 14 evidence for the charge transfer interactions [25,26].

The in-plane CH bending vibrations allowed by the asymmetrically tri-substituted phenyl rings are 3, 9b, 18b and 15 which are computed at 1295, 1148, 1082 and 1148 cm^{-1}, respectively which are in accordance with the previously reported vibrational assignments [27]. The wavenumbers of the above mentioned vibrational modes correlate with the

Table 4: Vibrational assignments of 2A-5CB based on potential energy distribution method

Calculated			Experimental		
ν_{calcm}^{-1}	Relative Intensity		$\nu_{IR\ cm}^{-1}$	$\nu_{Raman\ cm}^{-1}$	
	IR	Raman			Assignment with PED (%)[c]
3538	63	2	3418 vs	-	NH2 asy str(100)
3396	94	5	3314 vs	3315m	NH2 sym str(100)
3117	1	1	-	3191w	mode 2 of ring 1(99)
3098	7	4	-	-	mode 2e of ring2(95)
3097	7	5	-	-	mode 2 of ring 1(95)
3092	12	3	-	-	mode20a of ring 2(80)
3083	29	3	-	-	mode 20a of ring 2(87)
3073	10	4	-	-	mode 7b of ring 2(88)
3063	0	1	3063 w sh	3066vs	mode 20a of ring 2(87)
3061	16	3	-	-	mode 20a of ring 1 (95)
1638	110	18	1616 vs	1617vs	NH2 sci(11),C=Ostr(69)
1609	202	4	-	-	mode 8a of ring 1(44),NH2 sci(25)
1594	8	21	-	1596vs	mode 8a of ring 2(61)
1574	116	1	-	1575sh	NH2 rocking(22),mode 8b of ring 2(16)
1570	98	2	-	-	mode 8b of ring 2(24)
1534	112	9	1536 vs	1537vs	mode 19b of ring 1(27)
1479	3	1	-	-	mode 19a of ring 2(73)
1459	59	11	1466 w	1464s	mode 19a of ring 1(45)
1434	10	1	-	-	mode 19a of ring 2(63)
1398	17	6	1405 m	1410s	mode 14 of ring 1(59)
1326	11	3	-	1359m	mode 14 of ring 1(69)
1314	3	0	1318 s	-	mode 3 of ring 2(79)
1300	26	7	-	-	mode 3 of ring 1(63)
1295	17	1	1291 sh	1296m	mode 3 of ring 2(42),mode 3 of ring 1(29)
1275	89	1	-	-	mode 3 of ring 1(50)
1228	337	2	1238 s	1237w	C_4-C_5 str(11), C_5-C_{14} str(29), H_9-C_4-C_5 bend(22)
1167	23	1	1181 m	-	mode 9a of ring 2(89)
1149	4	3	-	-	mode 15 of ring 1(56), mode 15 of ring 2(12)
1148	29	2	1150 m	1153vs	mode 9b of ring 1(56),mode 9a of ring 2(66)
1123	30	26	-	-	C5-C14 str(19),mode 19a of ring 2(11), mode 19a of ring1(16)
1082	12	2	-	1097m	mode 18b of ring 1(69)
1072	6	0	-	-	mode15 of ring 2(78)
1039	6	1	-	1029m	H12- N11-C6 bend(44)
1016	3	6	-	1001s	mode 18a of ring 2(82)
979	2	10	-	-	mode 12 of ring 2(60)
965	0	0	-	-	mode 5of ring 2(81)
943	3	0	946 w	951w	mode 5 of ring 2(93)
926	46	1	-	925w	mode 17b of ring 1 (42),mode 17b

					of ring 2(15)
917	0	0	-	-	mode 17a of ring 1(82)
910	10	1	-	-	mode 10b of ring 2(56),mode 10b of ring 1(11)
884	12	1	889 w	888w	mode 10a of ring 1(78)
834	3	2	826s	833s	mode 10a of ring 2(87)
817	21	9	-	-	mode 10a of ring 1(36)
797	30	1	801 w	801w	mode 6 of ring 1(66)
786	10	1	762 w	766s	mode 10a of ring 1(20),mode 10a of ring 2(12), O_{26}-C_5-C_{15}-C_{14} out(31)
743	36	7	-	743w	mode 10a of ring1(13)
723	18	1	-	-	mode 10a of ring 2(27)
686	30	1	700 w	-	mode 11 of ring 2(84)
671	5	0	660 w	666m	mode 6b of ring 1(32),mode 6b of ring 2(13),O_{26}-C_5-C_{15}-C_{14} out(12)
648	37	3	644 w	648w	mode 6a of ring 1(11),mode 6a of ring 2(23)
636	20	1	-	618w	mode 6a of ring 1(43),C_3-Cl_{10} str(10)
608	0	3	-	-	mode 6b of ring 2(83)
591	69	2	-	562m	H_{12}-N_{11}-C_6-C_1 tor(75)
546	8	5	-	-	mode 4 of ring 1(22),mode 4 of ring 2(11)
513	17	1	520 m	-	mode 16b of ring 1(62)
454	8	4	468 w	467m	N_{11}-C_6-C_1 bend(60)
437	13	0	-	-	mode 16b of ring 1(49)
421	4	3	-	426m	mode 16b of ring1(33)
403	3	3	-	408sh	mode 16a of ring 2(86)
385	50	5	-	-	C_2-C_3-C_4 bend(36)
371	123	7	-	378m	C_3- Cl_{10}str(17), H_{13}-N_{11}-C_6-C_5 tor(42)
358	53	8	-	-	C_3-Cl_{10} str (26), H_{13}-N_{11}-C_6-C_5 tor(25)
312	4	1	-	323m	mode 16b of ring 1(60)
301	7	3	-	-	Cl_{10}-C_3-C_4 bend(60)
255	0	3	-	265m	C_5-C_{14} str(39)
218	1	10	-	227m	C_4-C_5-C_{14}- C_{15} tor(12), C_4-C_3- Cl_{10}(48)
175	1	9	-	190m	Cl_{10}-C_3-C_4 bend(18),C_{14}-C_{16}-C_{20}-C_{15} out(11),C_4-C_5-C_{14} bend(29)
129	3	9	-	149s	C_{14}-C_{16}-C_{20}-C_{15} out(66)
115	1	6	-	111vs	C_1-C_2-C_3-C_4 tor(79)
73	0	36	-	82 s	C_{14}-C_{16} -C_{20}-C_{15} out(38),C_4-C_3-Cl_{10} bend(30)
54	0	100	-	-	C_4-C_5-C_{14}-C_{15} tor(60),C_4-C_3-Cl_{10} bend(12)
39	1	34	-	-	C_1-C_2-C_3-C_4 tor(82)

vs-very strong; s-strong; m-medium; sh-shoulder; w-weak; vw-very weak; ring-phenyl ring; str-stretching; bend-bending; tor-torsion; sci-scissoring; wag-wagging; sym-symmetric; asy- asymmetric; out - out-of-plane bending

[c]Only PED values greater than 10% are given.

experimental values except the mode at 1148 cm^{-1}. The mode 3 is found to be a medium band in Raman at 1296 cm^{-1} and that in IR as a shoulder band at 1291 cm^{-1}. The mode 9b of ring1 is found to be strong in Raman at 1153 cm^{-1} and that in IR as a medium band at 1150 cm^{-1} (PED 56%) . The mode 18b of the ring1 is found only in Raman as a medium band at 1097 cm^{-1}. The normal modes 3, 9a, 5, 18a and 18b are classified as CH in-plane bending vibrations in mono-substituted benzene rings. The bands observed at 1291 cm^{-1} in IR and that at 1296 cm^{-1} in Raman are assigned to the mode 3 of Ph_2. The vibrational mode 9a is observed as a medium band in IR at 1150 cm^{-1} and Raman at 1153 cm^{-1} (PED 66%) as a strong band. The mode 18a occurs as a strong band in Raman at 1001 cm^{-1} (PED 82%).

The C-H out-of-plane bending of phenyl ring 1 are computed at 925 and 743cm^{-1} for 17b and 11 modes, respectively and the computed values correlate well with the experimental band positions showing that the C-H out-of-plane bending modes are less influenced by intermolecular interactions. The out-of-plane skeletal mode 6a of ring1 and 2 are found at 644 in IR and 648 cm^{-1} in Raman as weak bands. The C-H out-of-plane bending (5,10a, 10b, 11,17a), radial skeletal (1,12, 6a and 6b) and the out-of-plane skeletal (4,16a and 16b) of Ph2 vibrations are also listed in table 4.

C=O vibrations

The benzophenone skeleton forms the tripod that has C=O bond as one branch and other two branches are formed from phenyl rings. Because of the different electro-negativities of carbon and oxygen atoms, the bonding electrons are not equally distributed between the two atoms. The lone pair of electrons on oxygen also determines the nature of the carbonyl group [28]. In the vibrational assignments of aromatic and aryl aliphatic ketones, Kolev [29] observed the bands of í(C=O) for 14 different aromatic and aryl aliphatic ketones. The C=O stretching vibrations give rise to the characteristic bands in IR and Raman and the intensity of these bands can increase owing to the conjugation or formation of hydrogen bonds. The C=O stretching of ketones are expected in the region 1760-1730 cm^{-1}. A strong intense and well defined peak observed in Raman at 1617 cm^{-1} is due to the C=O stretching vibration of the carbonyl group. Similarly a highly intense band is observed at 1616 cm^{-1} in IR also due to C=O stretching (PED 69%). The lowering of C=O stretching wavenumber is due to the conjugation between the carbonyl group and the aromatic ring and also due to the formation of hydrogen bonding.

Amino group vibrations

The amino group is generally referred to as an electron donating substituent in aromatic ring system. The asymmetric interaction between the amino group and the aromatic ring produce a small displacement of the N-atom out of the benzene ring. In the region 3700-3300 cm^{-1}, only two bands are observed. The higher wavenumber band which is intense in the IR spectrum (3418 cm^{-1}) has been assigned to asymmetric stretching (PED100%) in amino group vibration. The intense band in IR spectrum (3314 cm^{-1}) and the medium band in Raman (3315 cm^{-1}) have been assigned to symmetric stretching (PED100%) of amino group vibrations. These assignments find support from the work of other researchers in the case of related molecules [30]. These wavenumbers and the ratio of intensities of the two bands are characteristic of NH_2 stretching mode. The lowering of NH stretching wavenumber is due to intermolecular N-H···O interaction. The red-shifting of wavenumber in the NH bond order value is occurring due to donor-acceptor interactions. The NH_2 stretching vibrations show the characteristic wavenumber shift caused by the halogen substituent also. Due to the low symmetry of the molecule, several internal coordinates also contribute to each normal mode. The NH scissoring deformation of amino groups appear around 1610-1630 cm^{-1} and the rocking deformation around 1070-1050 cm^{-1} [22]. The bands observed at 1617 and 1616 cm^{-1} in Raman and IR were assigned to the scissoring modes of NH_2 group. The band identified at 1575 cm^{-1} in Raman was assigned to the rocking mode.

CCl vibrations

The vibrations belonging to the bond between the ring and the halogen atoms are worth to discuss here, since mixing of vibrations are possible due to the lowering of the molecular symmetry and the presence of heavy atoms on the periphery of the molecule [31]. The assignments of CCl stretching and deformation vibrations have been made by comparison with similar molecules, *para*-bromophenol [32] and the halogen-substituted

benzene derivatives [33] assigned vibrations of C-X group (X=Cl, Br and I) in the wavenumber range of 1129-480 cm^{-1}. Normally the CCl stretching bands are expected around 1060-395 cm^{-1} [34]. In the 2A-5CB a weak Raman band at 618cm^{-1} is assigned to CCl stretching vibration. A medium band at 227 cm^{-1} (PED 48%) and a strong Raman band at 82 cm^{-1} (PED 30%) are assigned to CCl bending vibrations, which are coupled with C-C-C vibrations.

Nonlinear optical property analysis

Polarizability characterizes the ability of an electric field to distort the electronic distribution of a molecule. Higher order polarizabilities (hyperpolarizabilities β,γ) which describe the nonlinear response of atoms and molecules are related to a wide range of phenomenon from nonlinear optics to intermolecular forces, such as the stability of chemical bonds as well as the conformation of molecules and molecular aggregates [35]. These studies led to the fact that *ab initio* calculations of polarizabilities and hyperpolarizabilities have become available through the strong theoretical basis for analyzing molecular interactions. They made possible for the determination of the elements of these tensors from derivatives of the dipole moment with respect to the electric field. Since polarizabilities and hyperpolarizabilities are derivatives of the molecular energy with respect to the strength of the applied electric field, their theoretically calculated values may be sensitive to basis-sets and the levels of theoretical approach employed and the electron correlation can change the values of hyperpolarizabilities [36-40]. Even order hyperpolarizabilities are zero, vanishing for systems with inversion symmetry. However, in the present case the situation differs since, 2A-5CB is a non-centrosymmetric molecule possessing a permanent dipole moment, where the polarization response to an external electric field of fixed strength dominated by the π-electrons found that the origin of the nonlinearity is to be sought not only in the independent bonds formed by the ó electrons which contribute linearly, but in the delocalized ð electron cloud.

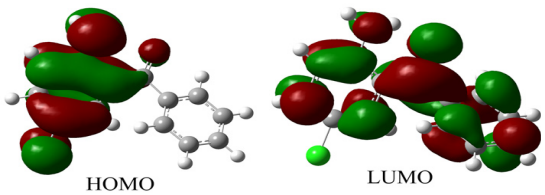

Fig. 5: HOMO and LUMO plots of 2A-5CB

The static hyperpolarizability (β_0) and it's related properties (β, α_0 and Δa) have been calculated on the basis of the finite-field approach. In the presence of an applied electric field the first-order hyperpolarizability is a third rank tensor that can be described by a 3 x 3 x 3 matrix. The components of b are defined as the coefficients in the Taylor series expansion of the energy in the external electric field. When the external electric field is weak and homogeneous, the expansion becomes.

$$E = E^0 - \mu_\alpha F_\alpha - 1/2\alpha_{\alpha\beta}F_\alpha F_\beta - 1/6\beta_{\alpha\beta\gamma}F_\alpha F_\beta F_\gamma + \ldots \quad \ldots(3)$$

where, E^0 is the energy of the unperturbed molecules, F_α is the field at the origin μ_α, $\alpha_{\alpha\beta}$ and $\beta_{\alpha\beta\gamma}$ are the components of dipole moment, polarizability and the first-order hyperpolarizability, respectively. From this, the first-order hyperpolarizability (β_0) using the x, y, z component is defined as

$$\beta_0 = (\beta_x^2 + (\beta_y^2 + \beta_z^2)^{1/2} \quad \ldots(4)$$

The calculated first-order hyperpolarizability of 2A-5CB is 1.53 x 10^{-30} e.s.u., which is 6 times greater than that of urea. From the computation, the high values of the hyperpolarizabilities of 2A-5CB are probably attributed to the charge transfer existing between the phenyl rings within the molecular skeleton. This is the evidence for nonlinear optical property of the molecule. The analysis of the wave function indicates that the electronic absorption corresponds to the transition from the ground to the first excited state and is mainly described by one-electron excitation from the highest occupied molecular orbital (HOMO) to the lowest unoccupied molecular orbital (LUMO). The atomic orbital compositions of the frontier molecular orbitals are sketched in Fig. 5. The HOMO energy=-8.19 eV, LUMO energy=-5.92 eV and HOMO-LUMO energy gap=2.2 eV. In addition, the decrease in HOMO and LUMO energy gap explains the eventual charge transfer interaction taking place within the molecule which is responsible for the NLO activity.

Analysis of organic molecules having conjugated ð-electron systems and large

hyperpolarizability using IR and Raman has been evolved as a subject of recent research [41]. The potential applications of 2A-5CB in the field of nonlinear optics demands the investigation of its structural and bonding features contributing to the hyperpolarizability enhancement by analyzing the vibrational modes using the IR and Raman spectra. The selection rule predicts the splitting of vibrational mode 19 (19a and 19b) in substituted phenyl rings. The modes 19a, 19b and 14 are active in both IR and in Raman simultaneously and their relative intensities are comparable which gives the evidence of the charge transfer from the donor to the acceptor group via the conjugated path, inducing charge variations in dipole moment and polarizability.

The C=O stretching vibrations give rise to the characteristic bands in the IR and Raman , and intensity of these bands can increase owing to the conjugation of formation of hydrogen bonds. The lowering of carbonyl stretching wavenumber is also contributed by the electron releasing effect of the C=O bond in the acceptor unit owing to intramolecular charge transfer as reported earlier [42] in addition to the intermolecular effect and ð-conjugation. Electron releasing effect in the C=O double bond causes polarizability change during vibration, making the Raman band also strong whose intensity is comparable to that of IR band.

CONCLUSION

The red-shift of the NH stretching wavenumber in the infrared spectrum indicates the presence of N-H···O bonding, resulting in proton transfer which increases the molecular hyperpolarizability of the material. The N-H···O hydrogen bonding network and the intramolecular charge transfer interaction has been analyzed using NBO analysis. The ð-electron delocalization over the carbazone moiety is responsible for the nonlinearity of the molecule. The simultaneous activation of the mode19 supports the charge transfer interaction. The calculated first-order hyperpolarizability of 2A-5CB is to be 1.53 x 10^{-30} e.s.u. The enhancement of hyperpolarizability value and the lowering of HOMO-LUMO energy gap confirms charge transfer interaction arise in the molecule.

ACKNOWLEDGEMENT

Prof. Micha³ H. Jamróz, Institute of Nuclear Chemistry and Technology, Warsaw, Poland for providing VEDA4 program.

REFERENCES

1. Vul, E.B.; Lobanova, G.M. *Kristallografiya*. **1967**, *12*, 411-413.
2. Fleischer, E.B.; Sung, N.; Hawkinson, S. *J. Phys. Chem.* **1968**, *72*, 4311-4312.
3. Babu, G.A; Thirupugalmani, K.; Jayaprakasan, M.; Ramasamy, P. *J. Cryst. Growth.* **2009**, *311*, 1607-1611.
4. Babu, G.A.; Ramasamy, P. *Mater. Chem. Phys.* **2010**, *119*, 533-538.
5. Genbo, S.; Shouwu, G.; Feng, P.; Youping, H.; Zhengdong, L. *J. Phys. D: Appl. Phys. B.* **1993**, *26*, 236-237.
6. Rauhut, G.; Pulay, P. *J. Phys. Chem.* **1995**, *99*, 3093-3100.
7. Frisch, M. J.; Trucks, G. W.; Schlegel, H. B.; Scuseria, G. E.; Robb, M. A.; Cheeseman, J. R.; Scalmani, G.; Barone, V.; Mennucci, B.; Petersson, G. A.; Nakatsuji, H.; Caricato, M.; Li, X.; Hratchian, H. P.; Izmaylov, A. F.; Bloino, J.; Zheng, G.; Sonnenberg, J. L.; Hada, M.; Ehara, M.; Toyota, K.; Fukuda, R.; Hasegawa, J.; Ishida, M.; Nakajima, T.; Honda, Y.; Kitao, O.; Nakai, H.; Vreven, T.; Montgomery, J. A., Jr.; Peralta, J. E.; Ogliaro, F.; Bearpark, M.; Heyd, J. J.; Brothers, E.; Kudin, K. N.; Staroverov, V. N.; Kobayashi, R.; Normand, J.; Raghavachari, K.; Rendell, A.; Burant, J. C.; Iyengar, S. S.; Tomasi, J.; Cossi, M.; Rega, N.; Millam, J. M.; Klene, M.; Knox, J. E.; Cross, J. B.; Bakken, V.; Adamo, C.; Jaramillo, J.; Gomperts, R.; Stratmann, R. E.; Yazyev, O.; Austin, A. J.; Cammi, R.; Pomelli, C.; Ochterski, J. W.; Martin, R. L.; Morokuma, K.; Zakrzewski, V. G.; Voth, G. A.; Salvador, P.; Dannenberg, J. J.; Dapprich, S.; Daniels, A. D.; Farkas, Ö.; Foresman, J. B.; Ortiz, J. V.; Cioslowski, J.; Fox, D. J. Gaussian, Inc., Wallingford CT, **2009**.

8. Becke, A.D. *J. Chem. Phys.* **1993**, *98*, 5648.
9. Lee, C.; Yang, W.; Parr, R.G. *Phys. Rev. B.* **1998***, 37*, 785-789.
10. Keresztury, G.; Chalmers, J.M.; Griffith, P.R. (Eds.), *Raman Spectroscopy: Theory, in: Hand Book of Vibrational Spectroscopy*, John Wiley and Sons Ltd., New York, **2002**.
11. Keresztury, G.; Holly, S.; Varga, J.; Besenyei, G.; Wang, A.Y.; Durig, J.R. *Spectrochim. Acta A* **1993**, *49*, 2007-2026.
12. Hoffmann, R.; Swenson, J.R.; *J. Phys. Chem.* **1970**, *74*, 415-420.
13. Akalin, E.; Akyüz, S. *J. Mol. Struct.* **1999**, *482*, 175-181.
14. Reed, A.E.; Curtiss, L.A.; Weinhold, F. *Chem. Rev.* **1988,** *88*, 899-926.
15. Foster, J.P.; Weinhold, F. *J. Am. Chem. Soc.* **1980**, *102*, 7211-7218.
16. Weinhold, F.; Landis, C.R. *Valency and Bonding: A Natural Bond Orbital Donor-Acceptor Perspective*, Cambridge University Press, New York, **2005**.
17. Thompson, H.W.; Torkington, P. *J. Chem. Soc.* **1945**, 640-645.
18. Glendening, E.D.; Badenhoop, J.K.; Reed, A.E.; Carpenter, J.E.; Bohmann, J.A.; Morales, C.M.; Weinhold, F. *NBO 3.1*, Theoretical Chemistry Institute, University of Wisconsin, Madison, **2001**.
19. Jamróz, M.H., *Vibrational Energy Distribution Analysis VEDA4*, Warsaw, **2004**.
20. Wilson, E.B. Phys. Rev. **1934**, *45*, 706-714.
21. Wilson, E.B.; Decius, J.C.; Cross, P.C. *Molecular Vibrations: The Theory of Infrared and Raman Vibrational Spectra*, Dover Publications, Inc., New York, **1955**.
22. Varsanyi, G., *Vibrational spectra of benzene derivatives*, Academic Press, New York, **1969**.
23. Ravikumar, C.; Hubert Joe, I.; Sajan, D. *Chem. Phys.* **2010**, *369*, 1-7.
24. Anjaneyulu, A.; Ramana Rao, G. *Spectrochim. Acta A*. **1999**, *55*, 749-760.
25. Ravikumar, C.; Hubert Joe, I.; Jayakumar, V.S. *Chem. Phys. Lett.* **2008**, *460*, 552-558.
26. Ravikumar, C.; Hubert Joe, I. *Phys. Chem. Chem. Phys.* **2010**, *12*, 9452-9460.
27. Green, J.H.S.; Harrison, D.J. *Spectrochim. Acta A* **1976**, *32*, 1265-1277.
28. Sathyanarayan, D.N., *Vibrational spectroscopy-theory and applications*, New age International (P) Ltd., New Delhi, **2004**.
29. Kolev, T. *J. Mol. Struct*., **1995**, *349*, 381-384.
30. Rostkowska, H.; Nowak, M.J.; Lapinski, L.; Bretner, M.; Kulikowski, T.; Leimage, A.; Adamowicz, L. *Spectrochim. Acta A,* **1993,** *49*, 551-565.
31. Yadav, R.A.; Sing, I.S. *Indian J. Pure Appl. Phys.* **1985,** *23*, 626-631.
32. Zierkiewicz, W.; Michalska, D.; Huyskens, T.Z. *J. Phys. Chem. A*, **2000**, *104*, 11685-11692.
33. Varsanyi, G., *Assignments for vibrational spectra of seven hundred benzene derivatives*, Adam Hilger, Mooney, **1974**.
34. Colthup, N.B.; Daly, L.H.; Wiberley, S.E., *Introduction to Infrared and Raman Spectroscopy*, Academic Press, London, **1964**.
35. Stephens, P.J.; Jalkanen, K.J. *J. Chem. Phys.* **1989**, *91*, 1379-1382.
36. Calaminici, P.; Jug, K.; Köster, A.M. *J. Chem. Phys.* **1998**, *109*, 7756-7759.
37. Colwell, S.M.; Murray, C.W.; Handy, N.C.; Amos, R.D. *Chem. Phys. Lett.* **1993**, *210*, 261-268.
38. McDowell, S.A.C.; Amos, R.D.; Handy, N.C. *Chem. Phys. Lett.* **1995**, *235*, 1-4.
39. Hermann, J. P.; Ricard, D.; Ducuing, J. *Appl. Phys. Lett.* **1973**, *23*, 178-181.
40. Tommasini, M.; Castiglioni, C.; Del Zoppo, M.; Zerbi, G. *J. Mol. Struct.* **1999**, *480*, 179-188.
41. Nakano, M.; Shigemoto, I.; Yamada, S.; Yamaguchi, K. *J. Chem. Phys.* **1995**, *103*, 4175-4181.
42. Delgado, M.C.R; Hernández, V.; Casado, J.; Navarrete, J.T.L.; Raimundo, J.-M.; Blanchard, P.; Roncali, J. *J. Mol. Struct.,* **2003**, *651*, 151-158.